Shape-Programmed Self-Assembly of Bead Structures

Cameron Nelson
Cornell University, College of Architecture, Art and Planning

Jenny Sabin
Cornell University, College of Architecture, Art and Planning

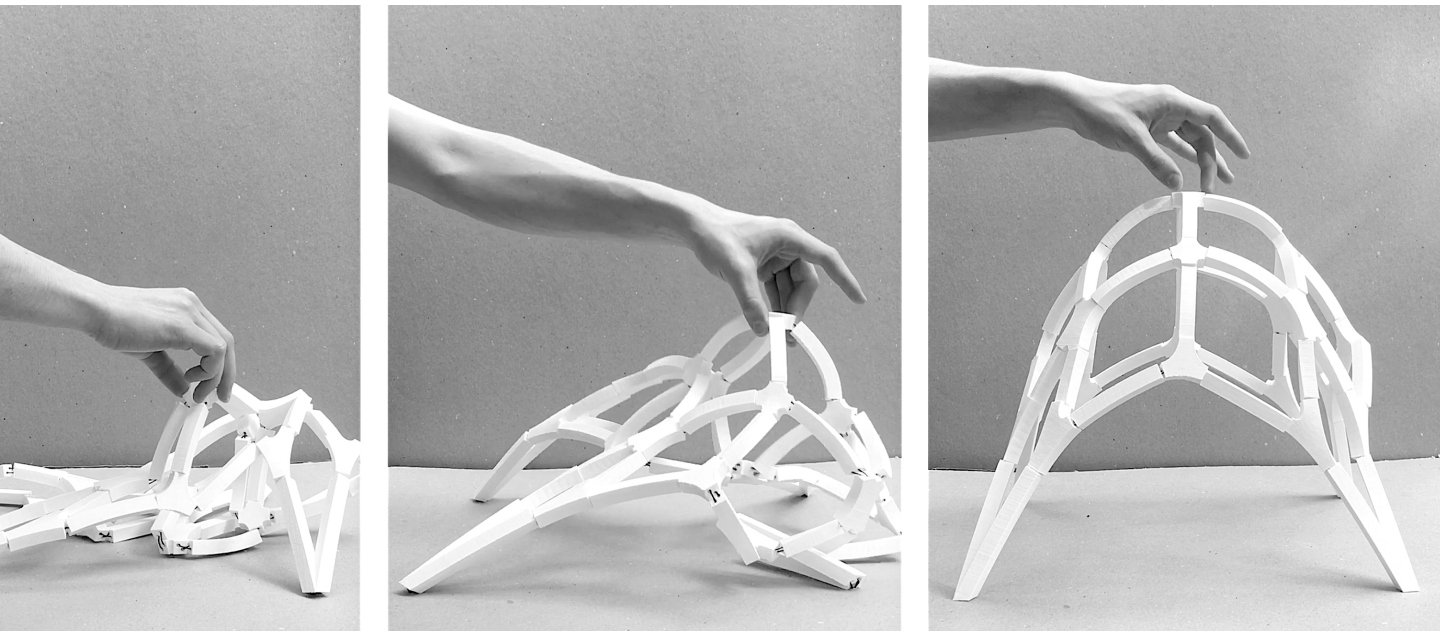

1

ABSTRACT

This paper demonstrates the potential of a robust, low-cost approach to programmable matter using beads and string to achieve complex shapes with novel self-organizing and deformational properties.

The method is inspired by the observation that beads forced together along a string will become constrained until they spontaneously rigidify. This behavior is easily observed using any household string and flat-faced beads and recalls the mechanism behind classic crafts such as push puppets. However, specific examples of architectural applications are lacking.

We analyze how this phenomenon occurs through static force analyses, physical tests, and simulation, using a rigid body physics engine to validate digital prototypes. We develop a method of designing custom bead geometries able to be produced via generic 3D-printing technology, as well as a computational path-planning toolkit for designing ways of threading beads together. We demonstrate how these custom bead geometries and threading paths influence the acquired structure and its assembly. Finally, we propose a means of scaling up this phenomenon, suggesting potential applications in deployable architecture, mortarless assembly of nonfunicular masonry, and responsive architectural systems.

1 A beadwork assembly can order itself into a self-standing structure with little to no aid.

2 Graph augmentation process. Left to right: framework, interfaces, and full solid geometry.

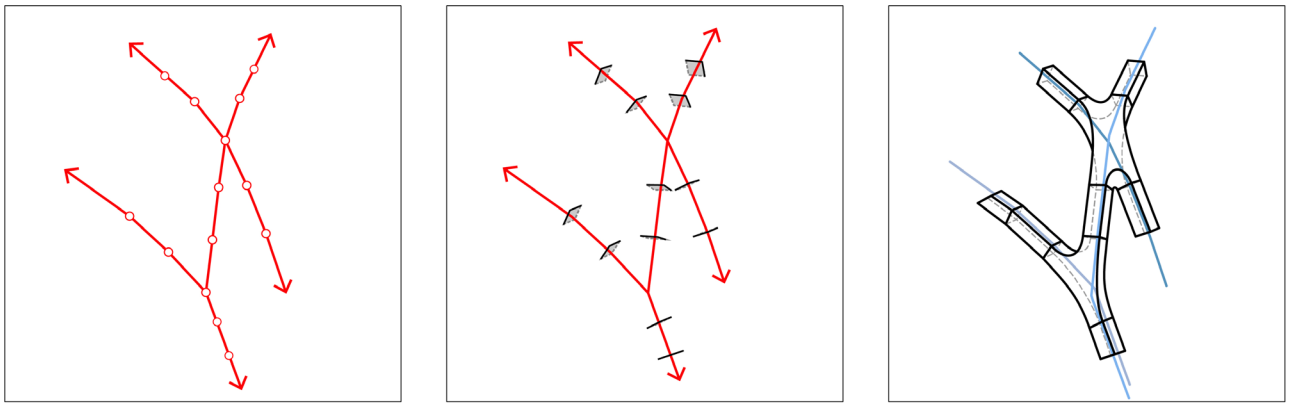

2

INTRODUCTION

Self-assembly at the microscale has been the subject of extensive biochemical research. This phenomenon has recently been shown to extend to the macroscale, as demonstrated by projects like Fluid Crystallization by MIT Self-Assembly Lab (Tibbits 2014). In such experiments, mimicking the biochemical example, components move freely in a fluid like air or water and are dependent on specialized "handshake mechanisms" like magnetic links. Related projects such as the Macrobot (Tibbits 2011) perhaps bear closer comparison with the present work, in that they encode a global geometry into a series of part-to-part rules. We consider the present work to be a continuation of this line of inquiry, deviating in its novel use of only tensile cord and solid geometry to achieve similar results without specialized components.

Research in lightweight, mortarless, tensegrity structures, such as the Periscope Tower by Matter Design Studio (Clifford and McGee 2011), offers further parallels. We seek to extend such examples, though, by applying tension dynamically, taking full advantage of the shape-changing qualities of flexural materials in addition to the structural qualities of rigid ones. Furthermore, beads as a tensegrity have the novel property of distributing compressive forces externally and tension internally, which contrasts with tensegrities commonly seen in deployable architecture such as inflatables and the iconic bar-and-cable systems of Kenneth Snelson and Buckminster Fuller.

Our work is also tangent to research in low-energy adaptive architectural systems, like TU Delft's Hyperbody "Muscle Tower II" (Bier 2011) and other large-scale prototype structures such as those built at University College, London (Senatore et al. 2017) and the University of Stuttgart (Sobek and Teuffel 2001). However, the focus of these projects is on control protocols for large batteries of actuators, rather than on the building components or structural units themselves, which tend to be traditional materials such as steel and standard mechanisms such as hydraulic pistons. Indeed, if the tensioning of the string in a beadwork structure is handled by pistons or other digitally controlled actuators, many of the same principles could be applied. On the other hand, bead structures are also versatile enough to be implemented as passive or human-powered systems, and can be designed, assembled, and upkept cheaply while still exhibiting qualities of adaptability and self-repair.

METHODS

Bead Shape

We considered beads to be solids with one or more hollow channels that may or may not intersect. This allows Y- and X-shaped beads (Fig. 2), as well as more complicated topologies. The most important aspect is the geometry of the contact surfaces, which determines orientation constraints and interlocking behavior as well as the torque between adjacent beads. For example, generic flat interfaces constrain position but not relative rotation, whereas interlocking interfaces can potentially fully constrain adjacent beads.

For complex geometries our design process begins from a skeletonized "framework": a connectivity graph with nodes embedded in 3D space. The edges of the graph are a placeholder for the network of string(s), which are added later. This is to be as generic as possible. In contrast with other workflows such as graphic statics, our choice of framework is essentially arbitrary, and need not necessarily reflect any kind of preoptimization or force analysis. For example, the geometry in Figure 6 is not a true

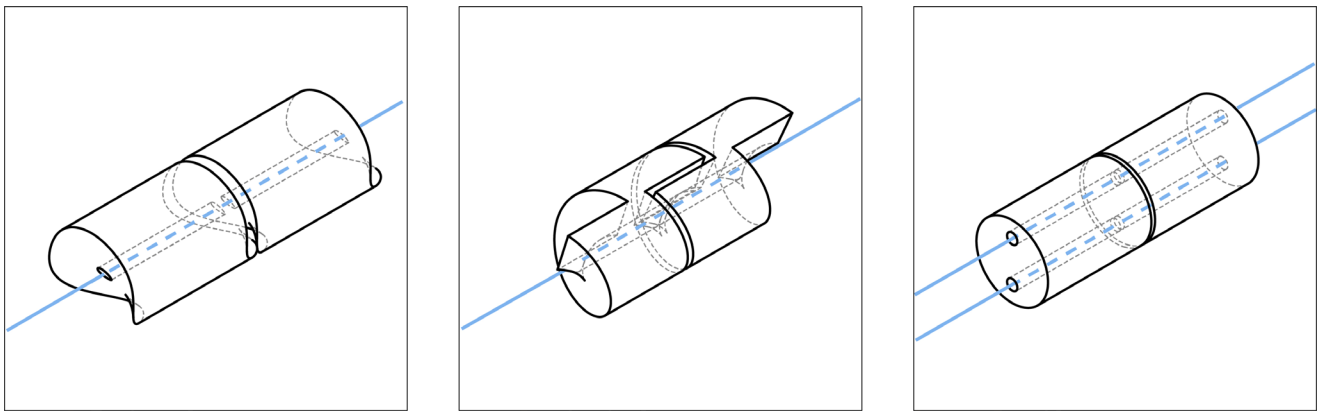

3

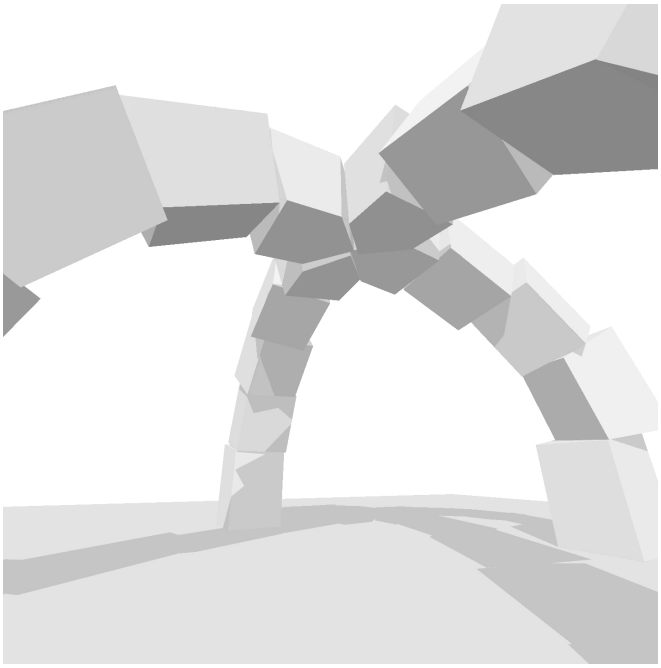

4

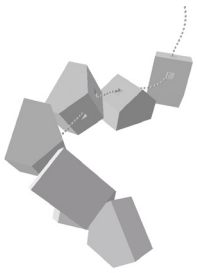

5a

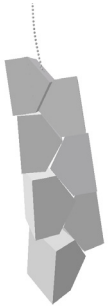

5b

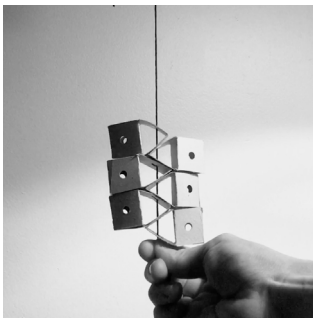

5c

3 Three possible bead geometries with different embedded intelligences. Left to right: lock-and-key, screw, and multicord joinery.

4 Still from rigid body simulation.

5 Simulation of bead shape that spontaneously arranges in an alternating pattern, (a) before, (b) after, and (c) physically.

funicular dome, and hence cannot stand without a tensile string holding the beads in compression. It would immediately collapse as a pure, mortarless masonry gridshell. Conceptually, the emphasis is not upon static form-finding to produce an ideal geometry at time of manufacturing but rather to produce a robust assembly that will weather unpredictable loading conditions and still return to its original state.

To generate printable bead geometries, we apply a method we term "graph augmentation": given a framework, we build volumetric beads about the edges such that the interface between two adjacent beads is aligned to the perpendicular plane of the edge between them in the framework (Fig. 2).

Relative orientation of beads can be shape-programmed by a variety of approaches, such as lock-and-key-type, screw-type, and multicord interfaces (Fig. 3). Bead orientations need not be maximally constrained to exhibit self-organization, however. For example, self-assembly of a regular 180° alternating pattern was observed in a simple 1D sequence of beads subject to agitation and gravity, in both physical tests and simulation (Fig. 5). We hypothesized we could use the same principle to create any angle of alternation, and with our simulation pipeline we were able to validate this intuition instantly.

Simulation

Dynamic architectural systems place unique demands on the designer to understand their behavior in time as

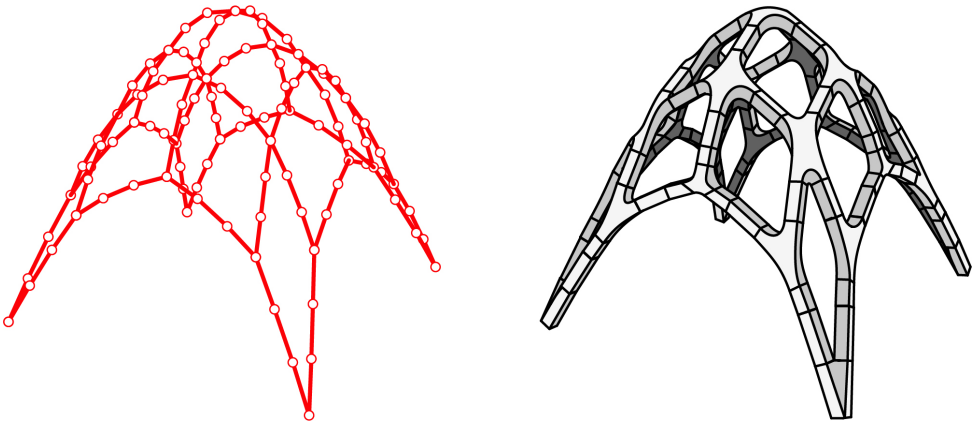

6 A complete generic dome framework (left) and the 3D printable bead geometries generated via graph augmentation.

6

a continuum and subject to a complex array of forces. Whereas physical scale models traditionally served this purpose, to mitigate rapid-prototyping turnaround times and quickly validate hypotheses we developed a pipeline from Rhino3d Grasshopper (Rutten 2020) to the physics engine Bullet (Fig. 4) (Coumans and Bai 2017). While this engine is primarily used for game physics and machine learning for robotics, its robust rigid-body collision physics makes it a natural choice for simulating string-bead interactions. String physics simulation methodologies generally fall into two categories: soft-body and rigid-body approximations. The latter approach treats a string as a chain of many small rigid bodies, each affixed to the next by a virtual joint. While soft-body approximations are specialized for deformable matter and may better simulate a string in isolation, simulations of beadwork are more reliable when strings and beads are approximated by the same type of object.

Thus, we treated a string as a chain of many small rigid bodies, each affixed to the next by a point-to-point constraint, since this approach has been validated for speed and accuracy (de Jong, Wormnes, and Tiso 2014; Gołębiowski et al. 2016). One difficulty in simulating beads and strings, especially when real-time interactivity is desired, is the computational burden produced by simulating collisions between concave mesh objects such as hollow beads. A standard workaround is to decompose each concave mesh into a series of convex parts whose collisions can be calculated much more quickly and accurately. Our simulation workflow employed both manual and automatic convex decomposition functionalities. General algorithms such as volumetric hierarchical approximate convex decomposition (VHACD) are widely used when geometry is not known beforehand (Mamou 2014). However, since our beads had predictable topology, we wrote custom convex decomposition scripts to yield more consistent and accurate results. Real-time interactivity in the simulations enabled invaluable feedback between *in silica* experiment, human understanding, and physical prototypes.

Threading Path

For any network topology more complex than a single row of beads in series, there may be many ways to thread them such that a cord passes through each bead at least once. For instance, we might use several threads each following a different path, and some beads might be threaded with multiple cords. There are many properties of a given threading path one might wish to optimize; here we consider (1) material economy, (2) ease of assembly, (3) shape control, and (4) mechanical effort.

Material economy: When the objective is to minimize the length of a single string, this reduces to the well-known Route Inspection problem (Edmonds and Johnson 1973). We implemented an algorithm using linear programming in the Python module PuLP (Mitchell and Dunning 2011), which solves this problem exactly. However, the threading paths can be highly asymmetric.

Ease of assembly: Often, when assembling a system by hand, a symmetrical threading path can be more intuitive to follow. The symmetries of a network are encoded in its automorphism group, a collection of ways of rearranging nodes of the graph such that path continuity is always preserved. By performing any such rearrangement on the vertices of a path, we obtain a topologically symmetric copy. The challenge then is to determine a set of one or more paths whose symmetric copies will cover the edges of the graph with the fewest overlaps. For example, in the threading diagram in Figure 15, there are only two unique paths that have been transformed into eight copies by a

7a

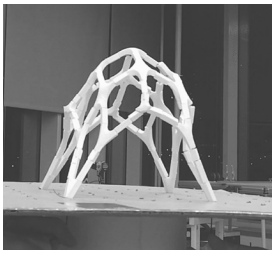

7b

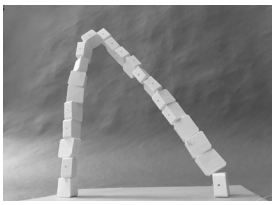

9a

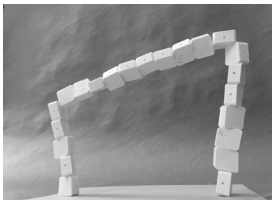

9b

8a

8b

7 Initial dome prototype: (a) before, and (b) after tensioning cord.

8 Tubular prototype exhibiting all X-type beads for greater geometric constraint. Self-repairing qualities are seen (a) before, and (b) after tensioning.

9 A simple indeterminate arch exhibiting multiple stable states (a–c) that appear more or less frequently in accordance with how they minimize a function of the kink angles; (d) shows a closeup of a kink.

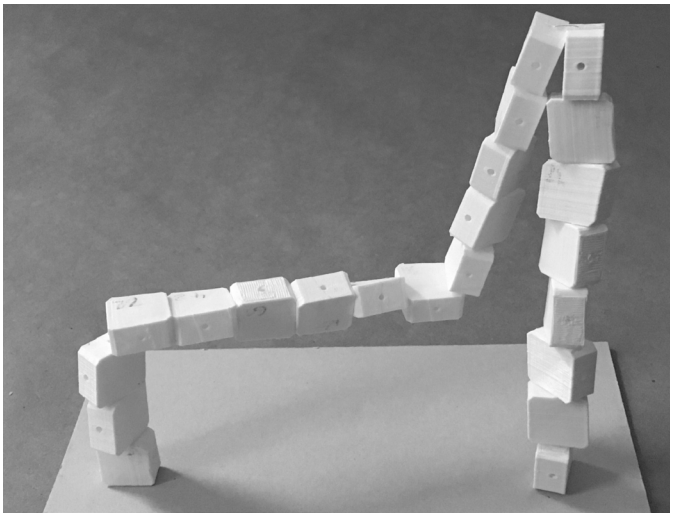

9c

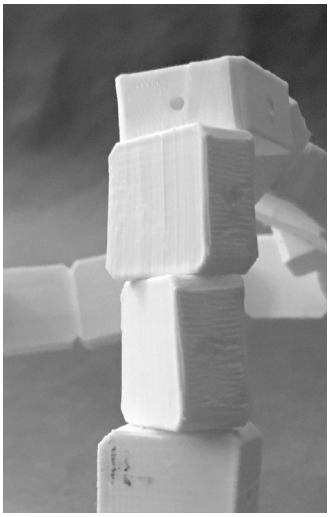

9d

subgroup of the graph's symmetries—in this case, the mirror symmetries. Unlike true mirror symmetry, though, graph automorphisms are topological in nature, making them robust to warping. This more generalizable approach to path planning can identify redundancy even in geometries that do not bear obvious symmetry.

Shape control: Geometric constraints upon one bead with respect to its neighbors can come not only from the bead's shape but also potentially from the threading pattern. As mentioned above and shown in Figure 3, multi-thread systems offer the benefit of constraining rotations. Two strings will fully constrain adjacent beads with planar interfaces, and three strings will fully constrain arbitrarily shaped beads, in the same sense that three points of contact are required to stabilize a chair. The dome model shown in Figure 1 exhibits a two-cord system with planar interfaces. A different approach to multicord threading patterns can be seen in the tubular prototypes in Figure 8. Here each bead represents a node of degree 4 in the model's graph representation. Thus, with a minimum of four points of contact per bead, the structure is fully constrained in position and orientation.

Mechanical effort: Minimizing the cumulative change in angle of a thread's path presents another possible criterion, since static analyses reveal that sharp angles can hinder force transmission by more than 70% (see "Static Force Analysis" below). Hence, less sharp angles will also minimize the force required to tension the bead system. In any network wherein all nodes are of even degree, we can break this problem into numerous smaller problems: for each node, we need to construct a matching among the incident edges such that the sum of the angles between matched pairs is minimized. This subproblem can be solved as a linear program, and if solved for each node independently, the resulting global threading path is guaranteed to minimize sharp turns in the threading path. In the special

11 Foam stereotomy could produce beadwork structures at larger scales, preserving volumetric shape programming while maintaining light weight. 11

case of a two-cord bead system, like those discussed above, all nodes have even degree by default. Even-degree frameworks also permit the use of the much simpler Fleury's Algorithm for generating an Euler Tour, which is a single path that crosses each edge in a graph exactly once, necessarily in the shortest possible way. Fleury's Algorithm, therefore, perfectly solves the Route Inspection problem for this special subcategory of frameworks.

These methods assume the existence of a static framework; however, one could also begin with a surface and place nodes and edges upon this surface in a manner conducive to more optimal threading paths. For example, a geodesic naturally minimizes the cumulative change in angle of a path between two points on a surface; hence a geodesic gridshell, though it may require many independent cords, compensates with a comparatively low activation energy. The tubular models in Figure 8 offer one example of this approach, as helices are geodesics on a cylinder.

RESULTS & DISCUSSION

Prototypes

We applied our techniques to a simple dome-shaped gridshell structure. The beads were 3D printed in generic polylactic acid (PLA) thermoplastic, and the threading was performed by hand with cotton cord. The first prototype had a footprint of approximately 5 in × 5 in. When the cords at each of the four feet were pulled, the beads spontaneously formed a rigid dome structure (Fig. 7). This success motivated a second prototype at approximately three times scale, with a 15 in × 15 in footprint, this time threaded such that two strings passed through each bead. This gave more control at the expense of increased friction. To compensate, the dome's assembly was minimally aided (Fig. 1). When tension was removed from the upright dome, the slightest touch would collapse the structure, demonstrating that this is not a true funicular dome but a tensegrity reliant on tension and compression in balance. Conversely, starting from a slack state, as the dome's apex was lifted into place simultaneously with a gradual reintroduction of tension, the remainder of the structure assembled of its own accord. This "one-handed" assembly behavior not only demonstrates the influence of threading path and friction on global behavior but also promises further use cases. For example, as a counterweighted window similarly retains its position after it is adjusted, a heavy structure could form and unform only with gentle assistance. This could potentially lead to a novel kind of masonry construction with improved safety, user-friendliness, and sustainability.

Analysis

Self-organization is a suggestive term used with varying definitions in the discipline of architecture. Inevitably there is some input energy, and even physical or biological definitions allow that this force may come from without the system itself, subtly augmenting the meaning of "self"-organizing. For example, Brownian motion is caused by particle bombardment, and in the Self-Assembly Lab's Fluid Crystallization project, a wave chamber is agitated to ensure intermixing of the floating magnetic modules (Tibbits

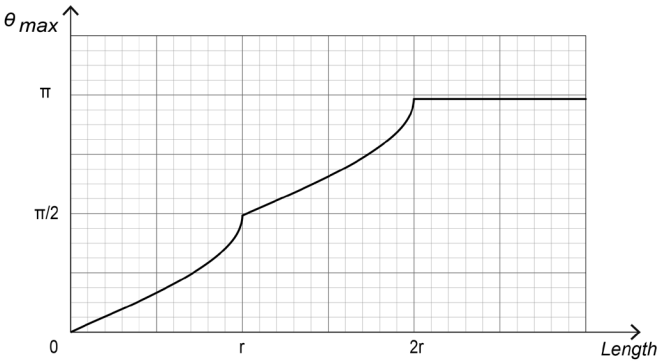

12

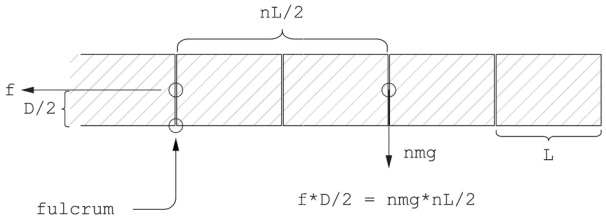

13

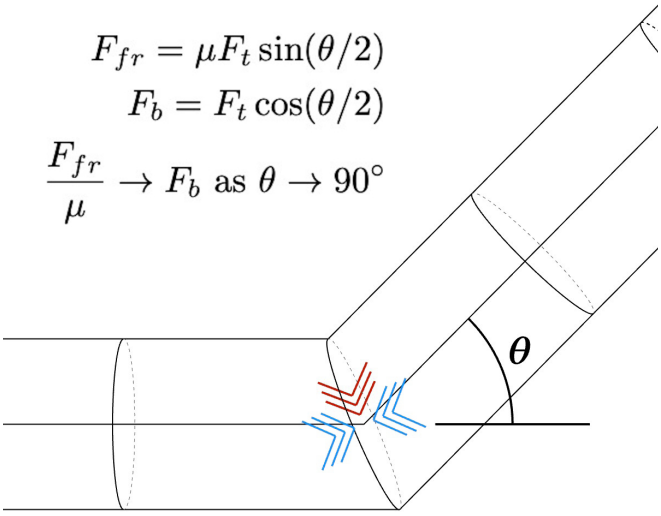

14

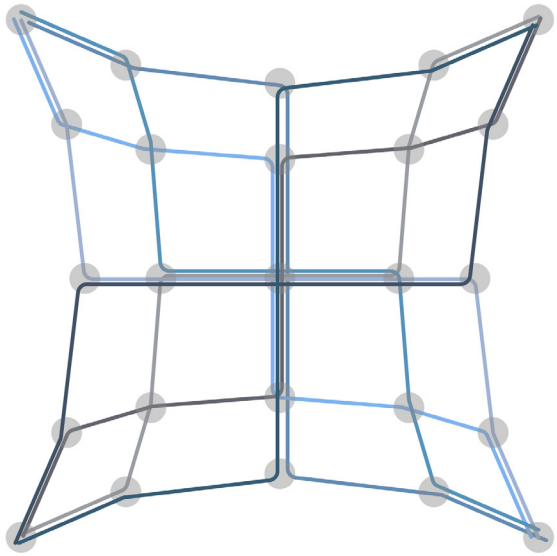

15

12 Maximum angle attainable between cylindrical beads as a function of the length of cord separating them. Note that $\theta_{max} \rightarrow 0$ as $l \rightarrow 0$, continuously but with discontinuous first derivative at $l = 2r$ and $l = r$. This graph illustrates the shrinking of the configuration space with the tensioning of the system.

13 The figure assumes a cantilever subjected to gravity. Bead diameter $D = 2r$ is inversely related to required tension f. L represents the bead length, m the mass per bead, and n the number of beads being supported. Because n is inversely proportional to both m and L, f is constant for changing n.

14 Two beads being compressed along a cord, demonstrating the effect of miter angle on friction between bead and cord. If θ is the supplement of the miter angle, $F_b = F_t \cos(\theta/2)$ and $F_{fr} = F_t \sin(\theta/2)$. For example, if $\theta = \pi/2$, we would expect $F_{fr} \approx 71\%F$.

15 A diagram of the threading path applied to the initial dome prototype (Fig. 7), as viewed from above. Here, symmetry is emphasized.

2014). Therefore, we adopt the interpretation that self-organization indicates an unordered form of agitation that nevertheless yields an ordered result. Inherent indeterminacy is, therefore, a hallmark of self-organization, by our definition.

A small "arch" model helps illustrate this principle (Fig. 9). Rather than a smooth arc, it forms a limited number of "kinks" in the sequence of beads. Repeatedly slackening and tensioning this arch, we observed that while the arch shape was different each time, certain arrangements of kinks were more likely to form in proportion with how much they minimized tension, or equivalently how much they maximized the angles at the joints. This probabilistic model strikes a balance between indeterminacy and order. Conversely, for a set of n kinks at specified positions in the sequence of beads, the angles formed at the respective kinks are consistently the same. We hypothesized that these angles are such that, if one views the arch as an n+1 bar linkage in the plane, then the sum of the squares of the angles between adjacent members is maximized.

In this example, "organization" can be quantified as the size of the system's configuration space, that is, the volume spanned by the valid domains in its parameter space. For example, we could measure the maximum angle between consecutive beads with respect to the distance separating their facing ends. If we define the length of cord between

the centers of two cylindrical beads' flat faces as l, the radius of the beads as r, and the maximum angle between the two beads' axes as θ_{max}, we obtain the set of equations below whose plot is shown in Figure 12, revealing a continuous monotonic decrease in θ_{max} as l decreases:

$$\theta_{max} = \begin{cases} \pi & \text{if } 2r \le l \\ \pi - \arccos((l-r)/r) & \text{if } r \le l \le 2r \\ \arcsin(l/r) & \text{if } 0 \le l \le r \end{cases}$$

In practice, this means that any shortening of the cord, such as by tension, will reduce the size of the configuration space until the system is forced into a constrained shape.

Static Force Analysis

In theory, using infinitely strong and frictionless materials, one can create a self-organizing bead structure approximating any given framework. In practice, however, friction, strength, and geometry play a role that can be limiting or fruitful. Consider the radius as the maximum distance from a point of contact between two beads to the string where it passes through them. A greater radius reduces the required tension force by supplying more torque. However, assuming constant density and cross-section, the aspect ratio of radius to length is unimportant. Figure 13 illustrates that n beads each l/n in length will require the same force to rigidify as m beads each l/m in length, for any n, $m > 0$.

Friction can significantly affect the transfer of tension. We observed this behavior even in relatively low-friction systems like the PLA and cotton-cord dome prototypes. In mitered beads like these, unlike in a straight chain of beads, the tension force applied to the cord is differently distributed, as seen in Figure 14. As the miter angle decreases, the normal force F_b between beads decreases, and the friction force F_{fr} between the string and the beads increases, requiring considerably greater force to pull.

Scale and Manufacturing

These considerations take on increasing importance as one begins to consider bead structures at larger scales. 3D printing has provided a natural means of producing these custom bead geometries, whose internal voids would present a challenge to most traditional subtractive manufacturing methods. In the interest of scaling bead structures to the human or building scale, novel materials and manufacturing methods ought to be considered. Using 3D-printed beads, but simply more of them, is one possibility. This offers the challenge of much more highly segmented frameworks, which become correspondingly more indeterminate as each vertex in the framework presents a potential for error, and this error may quickly accumulate into large displacements. Hierarchical approaches wherein substructures are rigidified incrementally could offer one solution.

A second approach is to use a large-scale volumetric material, such as foam, which offers high stiffness-to-density ratios. Precedents for large-scale foam tensegrities include the Periscope Tower by Matter Design Studio (Clifford and McGee 2011). This wind-prone structure was also stabilized by tension members, but differs from bead structures in that the cables were static and external to the foam blocks. Assuming traditional manufacturing methods of hot wire cutting and milling, which are less easily applied to complex concave surfaces, the challenge lies in how to run cords internally through a foam bead. One approach is to slice the bead along a plane through the desired thread path, then carve out half of the channel in each half of the bead before reassembling. To avoid the need for adhesives, the two halves of the bead can then be joined by wrapping with a secondary cord around the outer surface. This process of slicing and recombining recalls the "convex decomposition" process used to preprocess digital bead geometries for rigid body simulation, in a natural extension of the simulation-to-physical prototyping workflow. A visualization of what a large format bead test structure might look like is shown in Figure 11. Such a structure could provide rigid shelter while using no mortar and still be safe and robust to unusual loads such as high winds or children climbing upon it.

CONCLUSION

This preliminary study examined the potential of beads as a medium for controlled self-assembly and deployable structures. The potential applications of this technique are diverse, including but not limited to:

- rapidly deployable structures for disaster relief, temporary installations, and leisure.
- low-energy shape actuation for soft robotics and medical prosthetics, such as the CardioARM medical snake robot that uses a similar mechanism to control the joints of a many-segmented probe (Ota et al. 2009).
- assembly from a distance for autonomous structures in extreme environments as suggested by projects like MIT Self-Assembly Lab's Aerial Assembly project (Staback et al. 2017).

Rigid body simulation has also proven a valuable tool for rapid prototyping and experiment. The two prototypes presented in this paper demonstrate some potential

challenges of threading and scale that must be further investigated to validate these concepts for human-scale applications. Whereas graph augmentation offers a generic and versatile framework for design, further research should leverage our current understanding of forces and complexity to produce more robust specimens. Our approach to self-assembly is also virtually agnostic to the materials used. Even off-the-shelf materials are sufficient to demonstrate the behaviors discussed, but scaling up the combination of stiffness and lightness will place more constraints on the variety of suitable materials. In the context of existing research on self-assembly for architecture, though, this is a departure from the specialized handshake mechanisms heretofore seen, such as magnets, bimetals, shape-memory polymers, and thermo- or hygro-active materials. The self-assembly of beads offers a novel approach with potentially greater control of shape formation, tunable and reversible rigidity, and structural robustness.

ACKNOWLEDGMENTS

The authors would like to acknowledge the M.S. Matter Design Computation program of the Department of Architecture, Cornell College of Architecture, Art, and Planning, and the Sabin Lab at Cornell University.

REFERENCES

Bier, Henriette. 2011. "Robotic Environments." In *Proceedings of the 28th International Symposium for Automation and Robotics in Construction (ISARC)*, Seoul, South Korea, 29 June – 2 July 2011, 863–868. IAARC.

Clifford, Brandon, and Wes McGee. 2011. "Periscope Foam Tower." In *Fabricate 2011*, edited by Ruairi Glynn and Bob Sheil, 77–80. London: UCL Press.

Coumans, Erwin, and Yunfei Bai. 2018. *Pybullet*. https://pybullet.org/wordpress. V.2.88. PC.

Dear, Tony, Blake Buchanan, Rodrigo Abrajan-Guerrero, Scott David Kelly, Matthew Travers, and Howie Choset. 2020. "Locomotion of a Multi-Link Non-Holonomic Snake Robot with Passive Joints." *The International Journal of Robotics Research* 39 (5): 598–616.

de Jong, J., K. Wormnes, and P. Tiso. 2014. "Simulating Rigid-Bodies, Strings and Nets for Engineering Applications Using Gaming Industry Physics Simulators." Paper presented at *i-SAIRAS: International Symposium on Artificial Intelligence, Robotics and Automation in Space*, Montreal, June 17-19. European Space Agency.

Edmonds, Jack, and Ellis L. Johnson. 1973. "Matching, Euler Tours And the Chinese Postman." *Mathematical Programming* 5 (1): 88–124. https://doi.org/10.1007/bf01580113.

Gołębiowski, W., R. Michalczyk, M. Dyrek, U. Battista, and K. Wormnes. 2016. "Validated Simulator for Space Debris Removal with Nets and Other Flexible Tethers Applications." *Acta Astronautica* 129: 229–240. https://doi.org/10.1016/j.actaastro.2016.08.037.

Mamou, Khaled. 2014. *V-HACD: Volumetric-Hierarchical Approximate Convex Decomposition*. V.2.0. PC.
Mitchell, Stuart, and Iain Dunning. 2020. *PuLP: A Linear Programming Toolkit for Python*. V.2.0. PC.

Ota, Takeyoshi, Amir Degani, David Schwartzman, Brett Zubiate, Jeremy McGarvey, Howie Choset, and Marco A. Zenati. 2009. "A Highly Articulated Robotic Surgical System For Minimally Invasive Surgery." *The Annals of Thoracic Surgery* 87 (4): 1253–1256. https://doi.org/10.1016/j.athoracsur.2008.10.026.

Rutten, David. *Grasshopper*. V.1.0.0007. Robert McNeel & Associates. PC. 2020.

Senatore, Gennaro, Philippe Duffour, Pete Winslow, and Chris Wise. 2017. "Shape Control and Whole-Life Energy Assessment of an 'Infinitely Stiff' Prototype Adaptive Structure." *Smart Materials and Structures* 27 (1): 015022. https://doi.org/10.1088/1361-665x/aa8cb8.

Sobek, Werner, and Patrick Teuffel. 2001. "Adaptive systems in architecture and structural engineering." In *Smart Structures and Materials 2001: Smart Systems for Bridges, Structures, and Highways*, vol. 4330, pp. 36-45. International Society for Optics and Photonics, 2001.

Staback, Danniely, MyDung Nguyen, James Addison, Zachary Angles, Zain Karsan, and Skylar Tibbits. 2017. "Aerial Pop-Up Structures." In *ACADIA 2017: Disciplines & Disruption [Proceedings of the 37th Annual Conference of the Association for Computer Aided Design in Architecture (ACADIA) ISBN 978-0-692-96506-1]*, Cambridge, MA 2-4 November, 2017, 582–589. CUMINCAD.

Tibbits, Skylar. 2011. "A Model for Intelligence of Large-Scale Self-Assembly." In *ACADIA 11: Integration through Computation [Proceedings of the 31st Annual Conference of the Association for Computer Aided Design in Architecture (ACADIA) ISBN 978-1-6136-4595-6]*, Banff (Alberta) 13-16 October, 2011, 342-349. CUMINCAD.

Tibbits, Skylar. 2014. "Fluid Crystallization: Hierarchical Self-Organization." In *Fabricate 2014*, edited by F. Gramazio, M. Kohler, and S. Langenberg, 297–303. Zurich: UCL Press.

IMAGE CREDITS

All drawings and images by the authors.

Cameron Nelson received their BA in architecture and mathematics from Yale University. They are currently an MS candidate in the Matter Design Computation program at Cornell University College of Architecture, Art and Planning.

Jenny E. Sabin is the Arthur L. and Isabel B. Wiesenberger Professor in Architecture and Associate Dean for Design Initiatives at Cornell College of Architecture, Art, and Planning. She is the principal of Jenny Sabin Studio and director of the Sabin Lab at Cornell. Sabin holds degrees in ceramics and interdisciplinary visual art from the University of Washington and a Master of Architecture from the University of Pennsylvania. Her work has been exhibited at the FRAC Centre, Cooper Hewitt Design Triennial, MoMA, and the Pompidou. Sabin won MoMA & MoMA PS1's Young Architects Program with her submission, Lumen, 2017.